$e/3$ Laughlin Quasiparticle Primary-Filling $\nu = 1/3$ Interferometer

F. E. Camino, Wei Zhou, and V. J. Goldman

Department of Physics, Stony Brook University, Stony Brook, New York 11794-3800, USA

(Received 6 September 2006; published 15 February 2007)

We report experimental realization of a quasiparticle interferometer where the entire system is in 1/3 primary fractional quantum Hall state. The interferometer consists of chiral edge channels coupled by quantum-coherent tunneling in two constrictions, thus enclosing an Aharonov-Bohm area. We observe magnetic flux and charge periods h/e and $e/3$, equivalent to the creation of one quasielectron in the island. Quantum theory predicts a $3h/e$ flux period for charge $e/3$, integer statistics particles. Thus, the observed periods demonstrate the anyonic braiding statistics of Laughlin quasiparticles.

DOI: 10.1103/PhysRevLett.98.076805 PACS numbers: 73.43.Fj, 05.30.Pr, 71.10.Pm

A clean system of 2D electrons subjected to a high magnetic field at low temperatures condenses into fractional quantum Hall (FQH) fluids [1–4]. An exact filling f FQH condensate is gapped and incompressible. The celebrated examples of FQH condensates are the Laughlin many-electron wave functions for the *primary* fillings $f = 1/(2j + 1)$, with j an integer. The elementary charged excitations of a FQH condensate are the Laughlin quasiparticles. Deviation of the filling factor from the exact value is achieved by excitation of either quasielectrons or quasiholes out of the condensate, at such fillings the ground state of an FQH fluid consists of the quasiparticle-containing condensate. The FQH quasiparticles have fractional electric charge [2–6] and obey fractional statistics, that is, they are anyons [7–10].

Fractionally charged quasiparticles were first observed in quantum antidot experiments, where quasiperiodic resonant conductance peaks are observed when the occupation of the antidot is incremented by one quasiparticle [6,11,12]. A quantum antidot is a small potential hill defined lithographically in the 2D electron system. Complementary geometry, where a 2D electron island is defined by two nearly open constrictions, comprises an electron interferometer [13–16]. Recently, we reported the realization of a quasiparticle interferometer where $e/3$ quasiparticles of $f = 1/3$ fluid execute a closed path around an island of $f = 2/5$ fluid [9,10,17]. The interference fringes are observed as conductance oscillations as a function of the magnetic flux through the island, that is, the Aharonov-Bohm effect. The observed flux and charge periods, $\Delta_\Phi = 5h/e$ and $\Delta_Q = 2e$, correspond to excitation of ten $q = e/5$ quasiparticles of the 2/5 fluid. Such superperiodic $\Delta_\Phi > h/e$ had never been reported before in any system. The superperiod is interpreted as being imposed by the topological order of the underlying FQH condensates [18], manifested by the anyonic statistical interaction of the quasiparticles [19,20].

Our present experiment uses a similar quasiparticle interferometer, but with much less depleted constrictions, Fig. 1. This results in the entire island being at the primary filling $f = 1/3$ under coherent tunneling conditions, so that $e/3$ quasiparticles execute a closed path around an island of the 1/3 FQH fluid containing other $e/3$ quasiparticles. For the first time, we report interferometric oscillations in such devices. This simpler regime should help theoretical consideration of the quasiparticle interferometer physics. The observed flux and charge periods $\Delta_\Phi = h/e$ and $\Delta_Q = e/3$, respectively, correspond to the addition of one quasiparticle to the area enclosed by the interference path. These periods are the same as in quantum

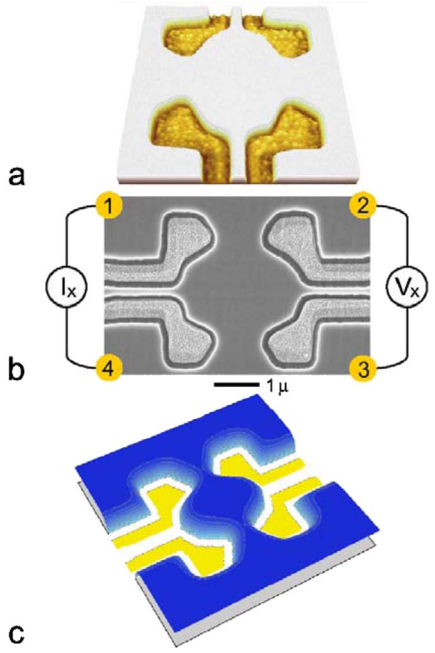

FIG. 1 (color online). The $e/3$ quasiparticle interferometer device. (a),(b) Atomic force and scanning electron micrographs. (c) Illustration of the 2D electron density profile. Four front gates are deposited in shallow etch trenches. Depletion potential of the trenches defines the electron island. The chiral edge channels follow equipotentials at the periphery of the undepleted 2D electrons. Tunneling occurs at the saddle points in the two constrictions. The edge channel path is closed by the tunneling links, thus forming the interferometer. The back gate (not shown) extends over the entire sample.

antidots, but the quasiparticle path encloses no electron vacuum in the interferometer. The results are consistent with the Berry phase quantization that includes both Aharonov-Bohm and anyonic statistical contributions.

Interferometer devices were fabricated from low disorder AlGaAs/GaAs heterojunctions. After a shallow 140 nm wet etching, Au/Ti front-gate metal was deposited in the etch trenches, followed by liftoff, Figs. 1(a) and 1(b). Samples were mounted on sapphire substrates with In metal, which serves as the back gate, and were cooled in a dilution refrigerator to 10.2 mK bath temperature, calibrated by nuclear orientation thermometry. Extensive cold filtering cuts the electromagnetic environment incident on the sample, allowing achievement of an electron temperature ≤ 15 mK in an interferometer device [21]. Four-terminal resistance $R_{XX} = V_X/I_X$ was measured with 50 pA ($f = 1/3$) or 200 pA ($f = 1$), 5.4 Hz ac current injected at contacts 1 and 4. The resulting voltage, including the interference signal, was detected at contacts 2 and 3.

The etch trenches define two 1.23 μm wide constrictions, which separate an approximately circular electron island from the 2D bulk. The shape of the electron density profile is largely determined by the etch trench depletion, illustrated in Fig. 1(c). Moderate front-gate voltages V_{FG} are used to fine tune the constrictions for symmetry of the tunnel coupling and to increase the oscillatory interference signal. For the 2D bulk density $n_B = 1.25 \times 10^{11}$ cm^{-2} there are $\sim$3500 electrons in the island. The depletion potential has saddle points in the constrictions, and so has the resulting density profile.

In a quantizing field B, counterpropagating edge channels pass near the saddle points, where tunneling may occur. Thus, in the range of B where interference oscillations are observed, the filling of the edge channels is determined by the saddle point filling [17]. This allows one to determine the constriction density from the $R_{XX}(B)$ and $R_{XY}(B)$ magnetotransport, Fig. 2(a). The Landau level filling $\nu = hn/eB$ is proportional to the electron density n, in a given B, the constriction ν is lower than the bulk ν_B. The island center n is estimated to be 3% less than n_B at $V_{\mathrm{FG}} = 0$, the constriction-island center density difference is $\sim$7%. Thus, the whole island is on the same plateau for strong quantum Hall states with wide plateaus, such as $f = 1$ and $1/3$. While ν is a variable, the quantum Hall exact filling f is a quantum number defined by the quantized Hall resistance as $f = h/e^2 R_{XY}$.

In the integer quantum Hall regime, the Aharonov-Bohm ring is formed by the two counterpropagating chiral edge channels passing through the constrictions. Backscattering occurs by quantum tunneling at the saddle points in the constrictions, Fig. 1, which complete the interference path. Relevant particles are electrons of charge $-e$ and Fermi statistics; thus, we can obtain an absolute calibration of the Aharonov-Bohm path area and the back-gate action. Figure 2(b) shows conductance oscillations for $f = 1$, similar oscillations also occur for $f = 2$. The

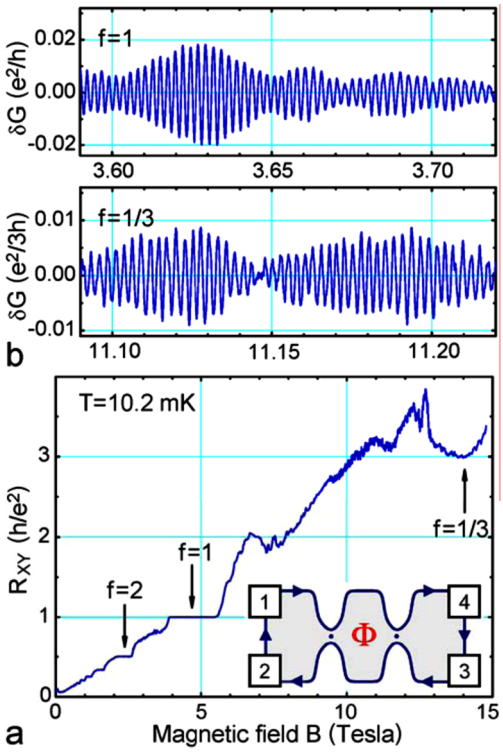

FIG. 2 (color online). (a) The Hall resistance of the interferometer device at zero front-gate voltage. The quantized plateaus allow one to determine the filling factor in the constrictions. Inset: the chiral edge channel electron interferometer concept; dots show tunneling. (b) Representative interference conductance oscillations for electrons, $f = 1$, and for $e/3$ quasiparticles, $f = 1/3$. The magnetic flux period is $\Delta_\Phi = h/e$ in both regimes. Negative front-gate voltage, applied to increase the oscillation amplitude, shifts the oscillations to lower B.

oscillatory conductance $\delta G = \delta R_{XX}/R_{XY}^2$ is calculated from R_{XX} data after subtracting a smooth background. The smooth background has two contributions: the bulk conduction at ν_B outside the bulk plateau regions, and the nonoscillatory interedge tunneling conductance in the interferometer. Extrapolated to $V_{\mathrm{FG}} = 0$ [14,17], the $f = 1$ magnetic field oscillation period is $\Delta_B = 1.86$ mT. This gives the interferometer path area $S = h/e\Delta_B = 2.22$ μm^2, the radius $r = 840$ nm.

In the FQH regime, we observe the interferometric oscillations on the low-B side of the $f = 1/3$ plateau, Fig. 2(b). This is the first experimental observation of $e/3$ quasiparticle interference oscillations when the island filling is $1/3$ throughout. Extrapolated to $V_{\mathrm{FG}} = 0$, the magnetic field oscillation period is $\Delta_B = 1.93$ mT. Assuming the flux period is $\Delta_\Phi = h/e$, this gives the interferometer path area $S = h/e\Delta_B = 2.14$ μm^2, the radius $r = 825$ nm. The island edge ring area is determined by the condition that edge channels pass near saddle points in the constrictions. Classically, increasing B by a factor of $\sim$3 does not affect the electron density distribution in the island at all. Quantum corrections are expected to be small for a large island containing $\sim$3500 electrons. Indeed, the

$f = 1/3$ interferometer path area is within $\pm 3\%$ of the integer value. Integer regime oscillations have an h/e fundamental flux period; we conclude that the flux period of $1/3$ FQH oscillations is also $\Delta_\Phi = h/e$.

We use the back-gate technique [6,11] to directly measure the charge period in the fractional regime. We calibrate the back-gate action $\delta Q/\delta V_{\mathrm{BG}}$, where Q is the electronic charge within the Aharonov-Bohm path. The calibration is done by evaluation of the coefficient α in

$$\Delta_Q = \alpha(\Delta_{V_{\mathrm{BG}}}/\Delta_B), \tag{1}$$

using the experimental oscillation periods, setting $\Delta_Q = e$ in the integer regime. Equation (1) normalizes the back-gate voltage periods by the experimental B periods, approximately canceling the variation in device area, for example, due to a front-gate bias. The coefficient α is known *a priori* to a good accuracy in quantum antidots because the antidot is completely surrounded by quantum Hall fluid [6,11]. In an interferometer, the island is separated from the 2D electron plane by front-gate etch trenches, so that its electron density is not expected to increase by precisely the same amount as n_B, requiring the calibration.

Figure 3 shows the oscillations as a function of V_{BG} for $f = 1$ and $1/3$ and the analogous oscillations as a function of B. At each filling, the front-gate voltage is the same for the (vs V_{BG}, vs B) matched set. The $f = 1$ period $\Delta_{V_{\mathrm{BG}}}$ corresponds to increment $\Delta_N = 1$ in the number of electrons within the interference path. We obtain $\Delta_{V_{\mathrm{BG}}} = 315$ mV, $\Delta_B = 2.34$ mT, and the ratio $\Delta_{V_{\mathrm{BG}}}/\Delta_B = 134.3$ V/T (front-gate $V_{\mathrm{FG}} = -210$ mV for these data). This period ratio is 0.92 of that obtained in quantum antidots [11], as expected. For the $1/3$ FQH oscillations, we obtain $\Delta_{V_{\mathrm{BG}}} = 117.3$ mV, $\Delta_B = 2.66$ mT, and the ratio $\Delta_{V_{\mathrm{BG}}}/\Delta_B = 44.1$ V/T (front gate $V_{\mathrm{FG}} = -315$ mV for these data). Using the integer calibration in the same device, the $e/3$ quasiparticle experimental charge period is $\Delta_Q = 0.328e$, some 1.7% less than $e/3$. To the first order, using the $\Delta_{V_{\mathrm{BG}}}/\Delta_B$ ratio technique cancels dependence of the V_{BG} and B periods on the interferometer area and front-gate bias. The scatter of the quasiparticle charge values obtained from several matched data sets is $\pm 3\%$ in this experimental run.

These experimental results can be understood as follows [16,22–24]: The experimental periods are the same as in quantum antidots, comprising the addition of one quasiparticle. When filling $\nu < 1/3$, as in quantum antidots, the addition of flux h/e to an area occupied by the $1/3$ condensate creates a quantized vortex, an $e/3$ quasihole. However, interferometric oscillations are observed to occur at filling $\nu > 1/3$, when quasielectrons are added to the condensate. This is consistent with the principal difference between the interferometer and the quantum antidots being that in antidots the FQH fluid surrounds electron vacuum, while the island contains the $1/3$ fluid everywhere within the interference path in the present interferometer. The addition of flux reduces the number of $-e/3$ quasielectrons, the electron system is not the same as prior to flux addition, the added flux cannot be annulled by a singular gauge transformation [25]. Another subtle difference is that a single quasihole can always be created in the $1/3$ condensate, while the creation of a single quasielectron is not energetically favorable in a large, weakly confined, *isolated* FQH droplet [24,26]. Periods of $\Delta_\Phi = 3h/e$ and $\Delta_Q = e$ have been predicted in certain $1/3$ FQH nonequilibrium models [16,22,23,27]. We therefore discuss experimental results via quasielectron configurations in the FQH ground state, as a more restrictive case.

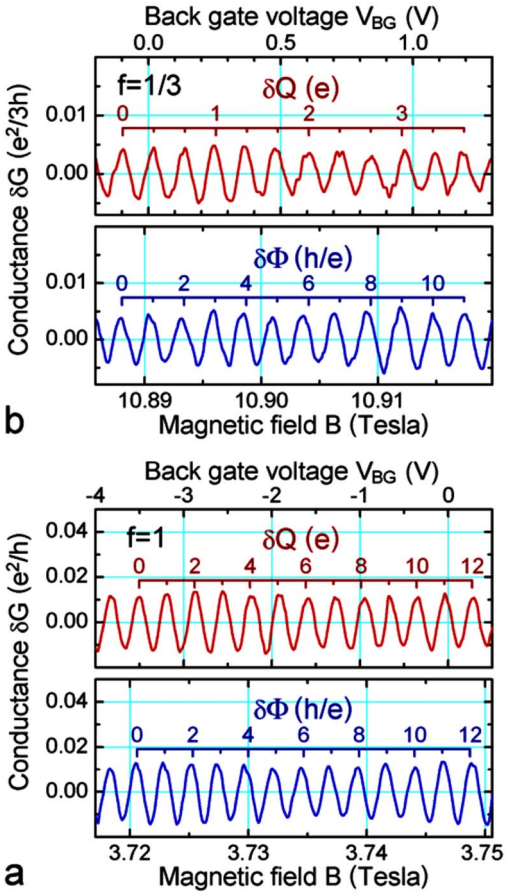

FIG. 3 (color online). Matched sets of oscillatory conductance data giving the $e/3$ charge period. (a) The interferometer device is calibrated using the conductance oscillations for electrons, $f = 1$. (b) This calibration gives the charge period for the Laughlin quasielectrons $q = (0.328 \pm 0.010)e$. The magnetic flux period $\Delta_\Phi = h/e$, the same in both regimes, implies anyonic statistics of the fractionally charged quasiparticles.

In an unbounded FQH fluid, changing ν away from the exact filling f is accomplished by the creation of quasiparticles; the ground state consists of $\nu = f$ condensate and the matching density of quasiparticles [3–5,24]. Starting at $\nu = f$, changing magnetic field adiabatically maintains the system in thermal equilibrium, exciting quasiholes ($\nu < f$) or quasielectrons ($\nu > f$) out of the exact filling condensate. The equilibrium electron density, deter-

mined by the positively charged donors, is not affected. Confining potential breaks the quasiparticle-quasihole symmetry of the 2D system. Thus, in the interferometer, when the current-carrying edge channel has $\nu = f$, the island center has $\nu > f$ because electron density is greater in the same B, consistent with experimental observation of oscillations on the low-B side of the $1/3$ plateau. Changing B also changes the flux $\Phi = BS$ through the area S enclosed by the interference path. In the experimental $\nu > 1/3$ regime, decreasing Φ by h/e increases the number of quasielectrons in S by one, $\Delta_N = 1$, and decreases by $+e/3$ the negative FQH condensate charge within S. The quasielectron is created out of the $1/3$ condensate, the condensate density changes by $+e/3S$, the charge within the interference path does not alter and still neutralizes the positive donor charge.

This process can be described in terms of the Berry phase γ of the encircling $-e/3$ quasielectron, which includes the Aharonov-Bohm and statistical contributions [8,24]. When there is only one quasiparticle of charge $q = \pm e/3$ present, its orbitals are quantized by the Aharonov-Bohm condition $\gamma_m = (|q|/\hbar)\Phi_m = 2\pi m$ to enclose flux $\Phi_m = mh/|q|$ with $m = 0, 1, 2, \ldots$. These quantized quasiparticle orbitals enclose $-em$ of the underlying $1/3$ condensate charge. When other quasiparticles are present, Berry phase quantization includes a term describing braiding statistics of the quasiparticles, in addition to the Aharonov-Bohm phase. The total phase is quantized in increments of 2π:

$$\Delta_\gamma = (q/\hbar)\Delta_\Phi + 2\pi\Theta_{1/3}\Delta_N = 2\pi, \qquad (2)$$

where $q = -e/3$ is the charge of the interfering quasielectron, and $\Theta_{1/3}$ is the statistics of the $-e/3$ quasielectrons. The first term in Eq. (2) contributes $(-e/3\hbar)(-h/e) = 2\pi/3$, the second term must contribute $4\pi/3$, giving an anyonic statistics $\Theta_{1/3} = 2/3$.

The same Berry phase equation describes the physically different process of the island charging by the back gate. Here, in a fixed B, increasing positive V_{BG} increases the 2D electron density. The period consists of creating one $-e/3$ quasielectron out of the $1/3$ condensate within the interference path, which causes the path to shrink by the area containing flux h/e. FQH fluid charge within the interference path does not neutralize the donors by $-e/3$. This is possible because the condensate is not isolated from the 2D bulk electron system, there is no Coulomb blockade, and the condensate charge within the interference path can increment by $+e/3$, any fractional charge imbalance ultimately supplied from the contacts. Thus, an $-e/3$ quasielectron is excited out of the condensate, $\Delta_N = 1$, the fixed condensate density is restored from the contacts, the interference path shrinks by area h/eB so that flux $\Delta_\Phi = -h/e$ in Eq. (2).

In conclusion, we realized a novel primary-filling $e/3$ quasiparticle interferometer where an $e/3$ quasiparticle executes a closed path around an island containing the $1/3$ FQH fluid only. The central results obtained, the flux and charge periods of $\Delta_\Phi = h/e$ and $\Delta_Q = e/3$ are robust. Both the Aharonov-Bohm and the charging periods accurately correspond to the excitation of one $-e/3$ quasielectron within the interference path and are consistent with fractional statistics theories of interacting FQH quasiparticles.

We acknowledge discussions with D. V. Averin and B. I. Halperin. This work was supported in part by the NSF and by U.S. ARO.

[1] D. C. Tsui, H. L. Stormer, and A. C. Gossard, Phys. Rev. Lett. **48**, 1559 (1982).
[2] R. B. Laughlin, Phys. Rev. Lett. **50**, 1395 (1983).
[3] R. B. Laughlin, Rev. Mod. Phys. **71**, 863 (1999).
[4] *The Quantum Hall Effect*, edited by R. E. Prange and S. M. Girvin (Springer, NY, 1990), 2nd ed.; D. Yoshioka, *The Quantum Hall Effect* (Springer, New York, 2002).
[5] F. D. M. Haldane, Phys. Rev. Lett. **51**, 605 (1983).
[6] V. J. Goldman and B. Su Science **267**, 1010 (1995).
[7] B. I. Halperin, Phys. Rev. Lett. **52**, 1583 (1984).
[8] D. Arovas, J. R. Schrieffer, and F. Wilczek, Phys. Rev. Lett. **53**, 722 (1984).
[9] F. E. Camino, W. Zhou, and V. J. Goldman, Phys. Rev. Lett. **95**, 246802 (2005).
[10] F. E. Camino, W. Zhou, and V. J. Goldman, Phys. Rev. B **72**, 075342 (2005).
[11] V. J. Goldman, I. Karakurt, J. Liu, and A. Zaslavsky, Phys. Rev. B **64**, 085319 (2001).
[12] V. J. Goldman, J. Liu, and A. Zaslavsky, Phys. Rev. B **71**, 153303 (2005).
[13] B. J. van Wees *et al.*, Phys. Rev. Lett. **62**, 2523 (1989); L. P. Kouwenhoven *et al.*, Surf. Sci. **229**, 290 (1990).
[14] F. E. Camino, W. Zhou, and V. J. Goldman, Phys. Rev. B **72**, 155313 (2005).
[15] C. M. Markus (private communication).
[16] C. de C. Chamon *et al.*, Phys. Rev. B **55**, 2331 (1997).
[17] W. Zhou, F. E. Camino, and V. J. Goldman, Phys. Rev. B **73**, 245322 (2006).
[18] X. G. Wen, Adv. Phys. **44**, 405 (1995); T. Senthil and M. P. A. Fisher, Phys. Rev. B **62**, 7850 (2000).
[19] J. M. Leinaas and J. Myrheim, Nuovo Cimento B **37**, 1 (1977).
[20] F. Wilczek, Phys. Rev. Lett. **48**, 1144 (1982); Phys. Rev. Lett. **49**, 957 (1982).
[21] F. E. Camino, W. Zhou, and V. J. Goldman, Phys. Rev. B **74**, 115301 (2006).
[22] S. A. Kivelson and V. L. Pokrovsky, Phys. Rev. B **40**, 1373 (1989).
[23] S. A. Kivelson, Phys. Rev. Lett. **65**, 3369 (1990).
[24] V. J. Goldman, Phys. Rev. B **75**, 045334 (2007).
[25] C. N. Yang, Rev. Mod. Phys. **34**, 694 (1962); R. B. Laughlin, Phys. Rev. B **23**, 5632 (1981).
[26] A. Cappelli *et al.*, Phys. Rev. B **58**, 16 291 (1998); E. V. Tsiper, Phys. Rev. Lett. **97**, 076802 (2006).
[27] Y. Gefen and D. J. Thouless, Phys. Rev. B **47**, 10423 (1993).